

Short communication

A conceptual model for explanation of Albedo changes in Martian craters

H. Xie^{a,*}, H. Guan^{a,b}, M. Zhu^{a,c}, M. Thueson^a, S.F. Ackley^a, Z. Yue^a

^aLaboratory for Remote Sensing and Geoinformatics, Department of Geological Sciences, University of Texas at San Antonio, San Antonio, TX 78249, USA

^bSchool of Chemistry, Physics and Earth Sciences, Flinders University, Australia

^cResearch Center for GIS and RS, East China Institute of Technology, Fuzhou, Jiangxi, China

Received 7 October 2007; received in revised form 15 December 2007; accepted 22 January 2008

Available online 23 February 2008

Abstract

We propose a conceptual model to interpret AM/PM high albedo events (HAEs) in crater interiors at the Martian seasonal polar caps. This model consists of two components: (1) a relatively permanent high-albedo water–ice body exposed in a crater interior and (2) a variable crater albedo in response to aerosol optical depth, dust contamination, and H₂O/CO₂ frost deposits or sublimates in four phases, based on temperature and solar longitude changes. Two craters (Korolev crater of fully exposed water–ice layer and ‘Louth’ crater of partially exposed water–ice layer) are used to demonstrate the model. This model explains the HAEs and their seasonal changes and suggests that many crater-like features formed in the last episodic advance of the polar ice cap in the last high obliquity period should have water–ice exposed or covered. For the AM-only HAEs craters, there seems no need of a water–ice layer to be fully exposed, but a subsurface water–ice layer (or ice-rich regolith) is a necessary condition.

© 2008 Elsevier Ltd. All rights reserved.

Keywords: Mars crater; High albedo event; Frost deposition and sublimation; Water–ice

1. Introduction

With increasing spacecraft exploration, our knowledge and understanding of Martian geology and climate is expanding. For example, there is consensus that the water–ice in the north polar cap is partially covered by CO₂ ice during the cold seasons, and totally uncovered during the warm seasons, while in the south polar cap, the majority of water–ice is normally covered by a thin bright CO₂ veneer in all seasons (e.g., Kieffer and Kieffer, 1976; Bibring et al., 2004, 2005; Byrne and Ingersoll, 2003; Titus et al., 2003); theoretically, one quarter of the CO₂ in the atmosphere above the north cap condenses in late summer each year (Leighton and Murray, 1966, Forget et al., 1998, Tillman et al., 1993).

The seasonal polar caps are a major element of the current Mars’ climate and circulation. Understanding the sublimation and condensation of CO₂ and H₂O is a key to

understanding recent, current, and future Martian climate and their seasonal changes, atmospheric circulation, and possibly the hydrological cycle. The impact craters or crater-like features at the seasonal polar cap regions, especially those associated with high-albedo deposits/events (HAEs) of ice and frost observed in late spring to summer seasons, provide a good opportunity to study H₂O and CO₂ condensation and sublimation. The high-albedo craters were first detected by the Viking Orbiter/MGS (Garvin and Frawley, 1998). Two prior hypotheses have been proposed to explain these HAEs in the literature.

One hypothesis is that these HAEs are a permanent residual ice in the craters, formed by either episodic advance of the polar cap margin (in the last high obliquity period) or continuous ice/dust deposits at high rates. This was proposed by Garvin et al. (2000) who used Mars orbiter laser altimetry (MOLA) data of Mars Odyssey to study the geometric characteristics of 15 icy craters (latitude 73–85°N). It is clear that: (1) they treated these HAEs as a permanent phenomenon in the associated craters or crater-like features; (2) based on limited data

*Corresponding author. Tel.: +1 210 458 5445; fax: +1 210 458 4469.

E-mail address: hongjie.xie@utsa.edu (H. Xie).

available during that time, it could not be determined that these HAEs have actual seasonal changes; and (3) it could not be determined if these HAEs are CO₂ and/or H₂O ice/frost. One discrepancy is that if the HAEs are due to continuous ice/dust deposits, then why does high-albedo ice/frost only appear at the central peak of the ‘Louth’ crater, but not over the crater floor (Xie et al., 2006)? In a normal case, the crater floor should have been favorable to receive more deposits than in the central peak. Also there are questions about the deposition rate. How large was it and how long did it take to deposit such an ice layer on a crater floor? Alternatively, an episodic advance of the polar ice cap in the last high-obliquity period could be an explanation, but it was not clearly described in their paper.

The other hypothesis is that these HAEs are newly formed water frost. Armstrong et al. (2005) studied the HAEs inside the Korolev crater (one of the 15 craters studied by Garvin et al., 2000) for its seasonal changes of albedo and bolometric temperature derived from thermal emission spectrometer (TES). They found that those HAEs do not seem to appear year round, but only during a period from early to middle summer. They suggest that the HAEs are newly formed water–frost, which was originally released from the extremely ice-rich layer (or regolith) in the subsurface of the crater interior and re-condensed/deposited on the crater floor. This explanation is similar to Bass et al. (2000), although Bass’s emphasis was not the crater ice but the entire residual polar region. Armstrong et al. (2007) further examined 60 craters (with diameter > 10 km) ranging from 60° to 90°N and found nine craters with AM-only (0140–0330 h local time) HAEs and nine craters with both AM and PM (1240–1420) HAEs (referred to as AM/PM hereafter). Their data show that all AM-only HAEs occur at temperatures below 200 K, while most AM/PM HAEs occur at temperatures above 200 K (200 K is the temperature for H₂O frost sublimation/condensation). For the AM-only HAEs, it is reasonable to explain that frost deposits (HAEs) in the evening and early morning (AM) are actively sublimating in afternoon due to high PM temperature, while it is difficult to explain the AM/PM HAEs. First, it requires much heavier evening and AM frost deposits, which could then be left and observed in the PM time even after sublimation. Since AM temperature for most of those HAEs craters was near or even a little higher than 200 K, it is impossible for significant water–frost deposit. Second, the explanation of Armstrong et al. (2005) and Bass et al. (2000) for those HAEs was the result of water–frost deposition, not of sublimation.

Overall, existing hypotheses provide clues for deciphering HAEs related to crater-like features in the Martian seasonal polar caps, but none gives a satisfactory and full picture to explain various HAE phenomena. With information from newly available high-resolution imagery, we propose a new conceptual model of H₂O/CO₂ frost sublimation/deposition process in craters or crater-like interiors, to explain the seasonal HAE phenomena.

2. Model description

The top part of Fig. 1 is the proposed conceptual model of sublimation/deposition of H₂O/CO₂ frosts related to a water–ice body exposed in a crater interior, with AM/PM HAEs. The bottom part of the figure consists of a TES-derived bolometric temperature (T) versus time (L_s) for the north polar region (latitude 86–87°N) (Titus, 2003), which approximately represents the T-trend of polar craters, and an ideal albedo profile based on TES-derived albedos of several water–ice bodies exposed in crater interiors, adapted to the temperature profile. It should be noticed that temperatures at lower latitudes will rise sooner and will reach even higher temperatures than shown in this profile. But the trend of temperature changes as L_s should be similar. For example, the temperature profile of Korolev crater (latitude of 72.8°N) has very similar trend as in Fig. 1, but rises sooner, reaches higher, and drops later, as expected. The model consists of two main components. (1) It requires a relatively permanent high-albedo water–ice

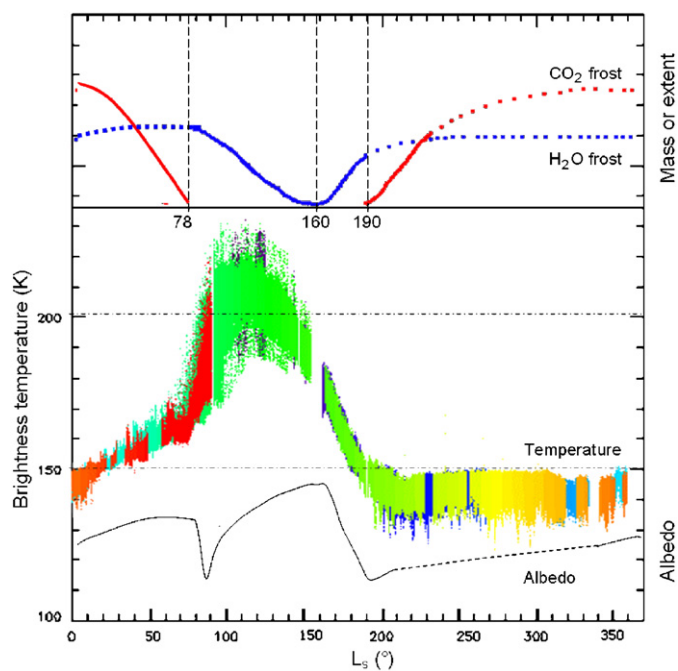


Fig. 1. Conceptual model of sublimation/deposition (or decrease/increase of mass or extent) of H₂O/CO₂ frosts related to a water–ice body exposed in a crater interior (top). Solid portions of the frost lines represent the major sublimation/deposition processes, while dotted portions are minor processes. Bottom part of the figure includes (1) a TES-derived bolometric temperature versus time (Titus, 2003), with sublimation/deposition lines of 150 K for CO₂ and 200 K for H₂O, conditioned on a typical atmospheric water column of 10 pr_{um}; and (2) an ideal albedo profile versus time (dotted portion is in the polar night) based on TES-derived albedos of several water ice bodies exposed in crater interiors, adapted to the temperature profile. Upper boundary of the temperature profile indicates the maximum temperature of PM time (1240–1420, local time), and lower boundary indicates the minimum temperature of AM time (0140–0330). The dark purple color of the TES temperature indicates the beginning of mapping orbit at $L_s = 104^\circ$. Green data indicate the end of the first year and the beginning of the second year. The red color data points indicate the most recently acquired data (Titus, 2003).

layer or patches exposed on part of or over an entire crater interior. It is assumed that polar caps once (in the last high-obliquity period) advanced to much lower latitude regions (at least 60°) and covered the floors of all bowl-like features that existed before the advance. When recession occurred, the ice left and survived on the crater floor because of the relatively low surface temperature inside those craters. Sediments from the cavity wall/rim and/or wind-blown dust/sand could then deposit on top of the water–ice, which resulted in partially ice-exposed crater (especially the deepest regions of the crater floor), no ice-exposed crater (especially small and deep ones), or fully ice-exposed crater (especially shallow and open ones). (2) For the craters with either a partial or full ice body exposed, the albedo changes as $\text{H}_2\text{O}/\text{CO}_2$ frosts either sublimed or deposited as detailed here:

Phase 1 ($L_s = 0\text{--}78^\circ$), a gradual increase of albedo could be mainly due to the decrease in aerosol optical thickness as sunrise over the polar region in the spring time (Vincendon et al., 2007; Langevin et al., 2007). The major process in the phase is CO_2 frost sublimation due to temperature increase over ~ 150 K. This results in decrease of CO_2 mass or extent.

Phase 2 ($L_s = 78\text{--}160^\circ$), at first there is a rapid decrease in albedo, which is then followed by a rapid increase. The decrease could be due to dust contamination after all the CO_2 frost sublimation; as temperature continues to rise up, dust could thermally sink into the water–ice and/or fall into cracks between larger grains of water–ice (Langevin et al., 2005). This will result in albedo increase (Vincendon et al., 2006, 2007; Langevin et al., 2005). In the same time, H_2O frost starts sublimation as temperature rising up over 200 K. The dominant process of this phase is the H_2O frost sublimation during the afternoon time, i.e. decrease of water–frost/ice mass or extent.

Phase 3 ($L_s = 160\text{--}190^\circ$), decrease of albedo could be due to a mixed effect of exposing old water–ice (larger grain size, e.g. $700\text{--}800\ \mu\text{m}$ as shown by Langevin et al., 2005) and increased aerosol thickness caused by dust storm during the period (Vincendon et al., 2007; Hale et al., 2005; Cantor et al., 2001). In the same time, deposition of fine grain H_2O frost starts as temperature decreases down to below 200 K. The fine grain H_2O frost usually has higher albedo. But this does not change the overall albedo decrease. Major process occurring in this phase is the increase of water–ice/frost mass or extent:

Phase 4 ($L_s = 190^\circ\text{--}360^\circ$), gradual increase of albedo due to the deposition of CO_2 frost. The major process in this phase is the increase of CO_2 mass or extent (maybe a slight increase of H_2O mass or extent as well), with CO_2 frost eventually covering the H_2O ice/frost and the rest of the area.

The exact timing of each phase and magnitudes of temperature and albedo could change from crater to crater depending on temperature, which is determined by crater elevation, depth, diameter, and locations (especially latitude), although the basic trend and phases should be

similar. The relatively permanent exposure of water–ice mentioned above means (a) at least tens of thousands of years and (b) dynamic processes of ice and frost sublimation and deposition, plus dust deposition.

3. Examples to demonstrate the model

We have examined most of the 18 craters (9 AM/PM craters and 9 AM-only craters) mentioned by Armstrong et al. (2007) and some others mentioned by Garvin et al. (2000) for the model development. In this paper, we are only using two of them as examples: a fully ice-exposed crater and a partially ice-exposed crater, to demonstrate the proposed conceptual models.

3.1. Korolev crater (72.8°N and 164.6°E)

TES-derived albedo and temperature profiles versus time of the crater interior are shown in Fig. 2 (from Armstrong et al., 2005), which have similar trends as the conceptual model illustrated above, except for the different starting and ending times of each phase. The albedo can be summarized based on the four phases. The albedo gradually increases from 0.37 to 0.48 (Phase 1: $\sim 0\text{--}50$); decreases first (to ~ 0.3) and then increases to ~ 0.55 (Phase 2: $\sim 50\text{--}160$); decreases again to ~ 0.24 (Phase 3: $\sim 160\text{--}200$); and then gradually increases again to ~ 0.37 (Phase 4: $\sim 200\text{--}360$). Armstrong et al. (2005) explained that the water–frost deposition was the reason for the albedo increase from early to middle summer (here Phase 2), while the water–frost originally came from the extremely ice-rich subsurface layer in the crater. They did not clearly state when the sublimation and deposition occurred. But from the TES temperature profiles, it seems impossible to deposit water–frost during the afternoon (PM) in early to middle summer time, while the HAEs are observed at both PM and AM. A previous study (Kieffer and Titus, 2001) suggested water vapor sublimated from an ice-rich layer within the crater during early summer, recondensed and deposited on the surface in later summer. This process does not explain why the HAEs occur in later spring and early summer.

Fig. 3 shows available THEMIS visible images of the crater as L_s increase. Water–ice does not appear in the winter ($L_s = 349.5^\circ$) and early spring images (17.9°) since there is not much albedo difference between inside and outside the crater, with some cases, inside albedos even slightly lower than outside albedos. This is the time when temperature is less than 150 K and CO_2 frost covers the entire area including the water–ice inside the crater. From later spring ($L_s = 85.3^\circ$) to later summer ($L_s = 164^\circ$), the interior albedos are higher than those of the exterior, which clearly indicates that a water–ice body almost completely covers the crater floor. This is also clearly seen in the MOC time series imagery (Fig. 4). We believe there is a relatively permanent water–ice body (‘ice lake’) exposed on the crater floor. This water–ice body was left after the last recession

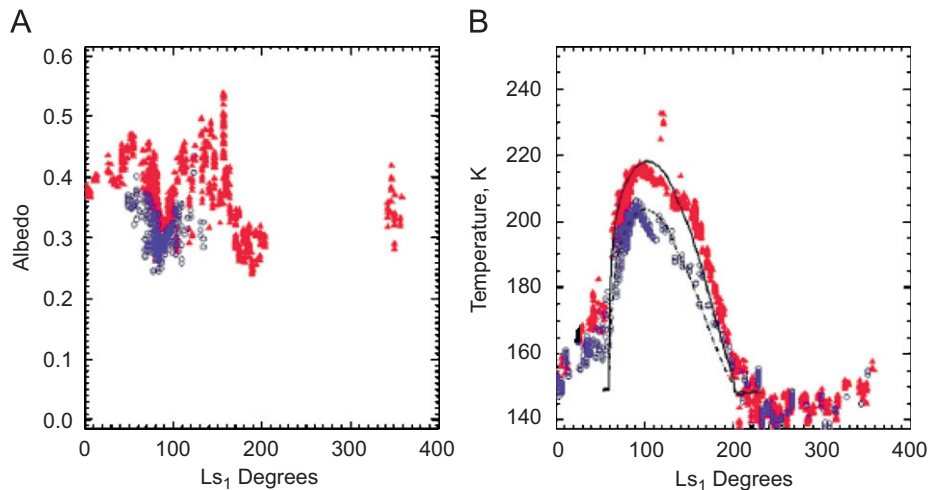


Fig. 2. TES derived albedos (left) and bolometric temperature (right) for both PM (red) and AM (blue) measurements for the interior of Korolev crater. Solid (PM) and dashed lines (AM) are model results (*source: Armstrong et al., 2005*).

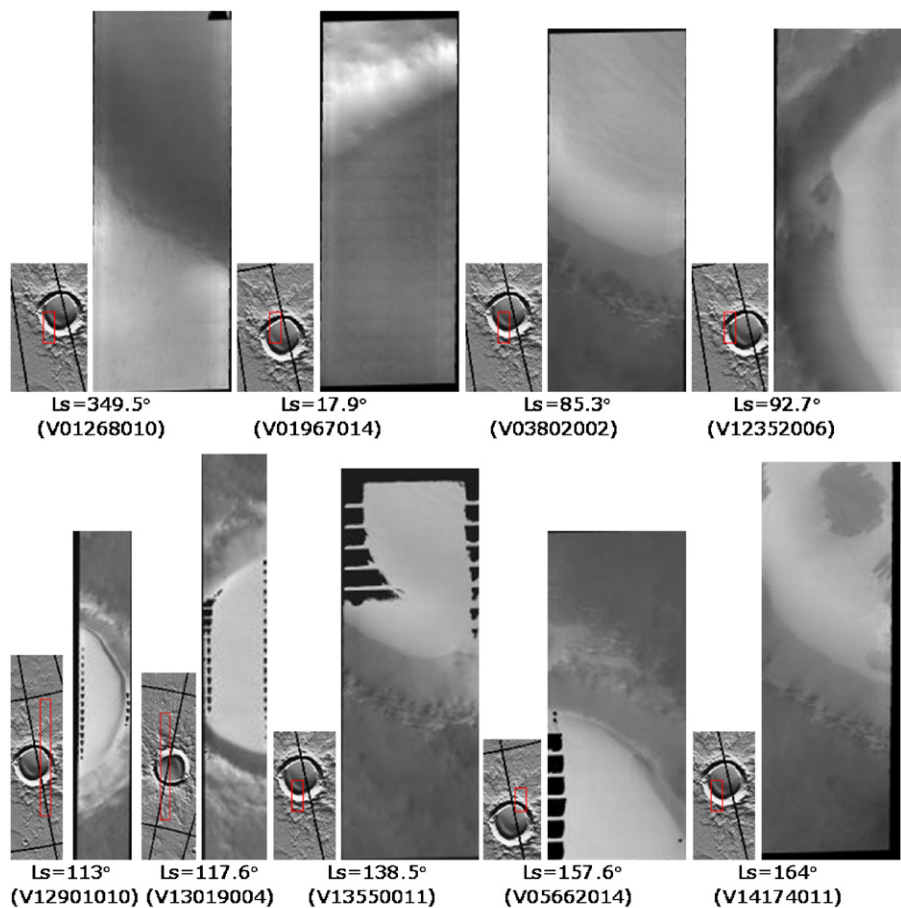


Fig. 3. Time series THEMIS visible imagery (with each pair consisting of a footprint map and the image) of the Korolev crater. HAEs was first seen at $L_s = 85.3^\circ$.

of the polar ice cap during the last high-obliquity period. The erosion of the crater rim and wall as well as dust deposits have not fully covered the water-ice yet, instead, have become a part of the water-ice, forming a so-called “dirty ice” upper layer. Spectra from OMEGA

have undoubtedly identified these high-albedo materials as water-ice (Langevin et al., 2005). Their paper also showed a best model fit of surface dust contamination to the water-ice; decrease from 9% ($L_s = 93.6^\circ$) to 5% ($L_s = 107.4^\circ$), which is suggested as a major reason for

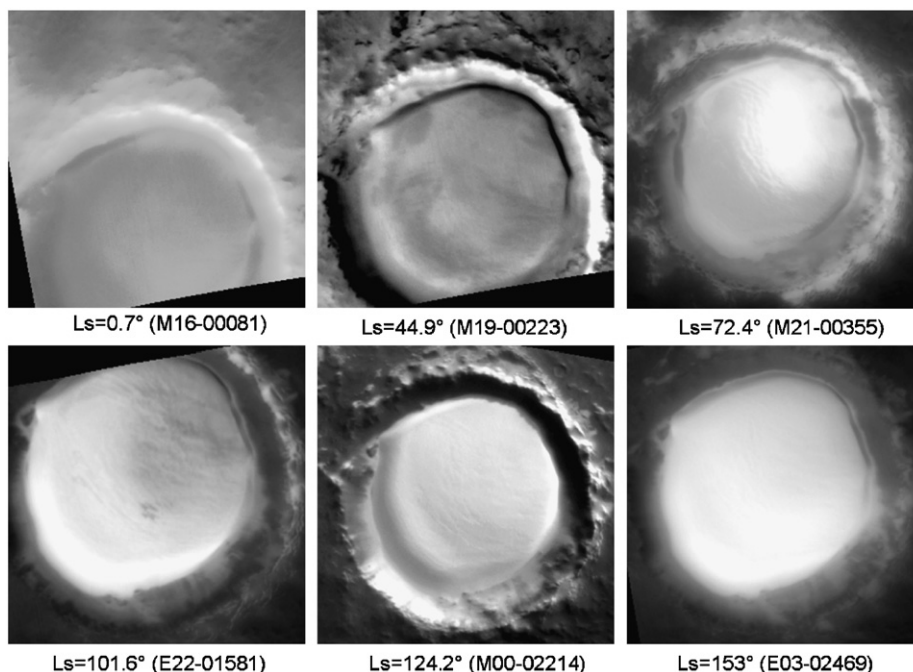


Fig. 4. Time series MOC wide-angle imagery of the Korolev crater (80 km in diameter). HAEs was first seen at $L_s = 72.4^\circ$.

albedo increase. The decrease of dust was due to thermally sinking into the water–ice and/or falling into cracks between larger grains of water–ice. There is no need for water–frost deposition to increase the albedo in this period (Phase 2) and the PM temperature of over 200 K does not allow the water–frost deposition in the PM time. Besides that the crater matches very well with the four phases of proposed conceptual model, the water–frost re-deposition during the night time could be started as early as $L_s = 130^\circ$ as shown by Armstrong et al. (2005). It is interesting that several low-albedo patches (crater floor materials) were seen from the water–ice body in the THEMIS image at $L_s = 164^\circ$ (2/23/2005). This is in the early stage of phase 3, after a complete sublimation of H_2O frost as well as some old water–ice (i.e., large grain size over $700 \mu\text{m}$ as modeled by Langevin et al., 2005) in phase 2. This suggests that the water–ice body itself in this crater is not so thick in the areas where the low-albedo materials were exposed. These low-albedo patches were not seen in the MOC image at $L_s = 153^\circ$ (4/29/2001) in a similar season but during a different year. This suggests that the exposure of the low-albedo patches is probably a temporal and local event, and that these low-albedo patches could be soon covered by water–frost deposition and later CO_2 frost deposition, starting another annual cycle. If the mass of H_2O frost deposits is less than the sublimation, the areas where low-albedo materials exposed could become larger and larger, and eventually the entire water–ice body could be sublimed away. Without the water–ice as a sublimation source, the annual cycle of albedo change inside the crater would be significantly different than it is at present. Further and detailed monitoring of the crater is therefore strongly recommended

to operational teams of the Mars Express and Mars Reconnaissance Orbiter (MRO).

3.2. ‘Louth’ crater (70.5°N and 103.2°E , officially unnamed)

A water–ice layer in this crater was first reported through the HRSC (imaged on 2/2/2005 ($L_s = 153.7^\circ$)) on board ESA’s Mars Express spacecraft. A preliminary analysis based on THEMIS visible and thermal data found that the major HAEs only appear on the central peak of the crater in both AM and PM during late spring to late summer seasons (Fig. 5—left) (Xie et al., 2006). Three THEMIS PM brightness temperature images were examined (Fig. 5-right). The one in the early spring ($L_s = 33.4$) does not show any temperature difference between the central peak and the rest of the floor. The one in the later spring ($L_s = 71^\circ$) shows that (1) temperature ranges from 214 to 246 K, meaning that water–frost/ice was in a sublimation process during the PM time; and (2) average temperature of the water–ice in the central peak was ~ 222 K, 18 K lower than the average temperature of the crater floor free of water–ice. If only a thin layer of water–frost (not a water–ice layer) existed in the central peak, the HAEs may not last long enough due to the high temperature. The AM brightness temperature image ($L_s = 137.4^\circ$) shows that the temperature ranges from 180 to 195 K, below the water–frost condensation temperature. This suggests that it is possible for water vapor, originating from sublimation during PM time, to re-condense and deposit during AM time. This is possibly the reason why we see faint traces of water–frost along the rim of the crater and on the crater walls in the HRSC image (Fig. 5—left).

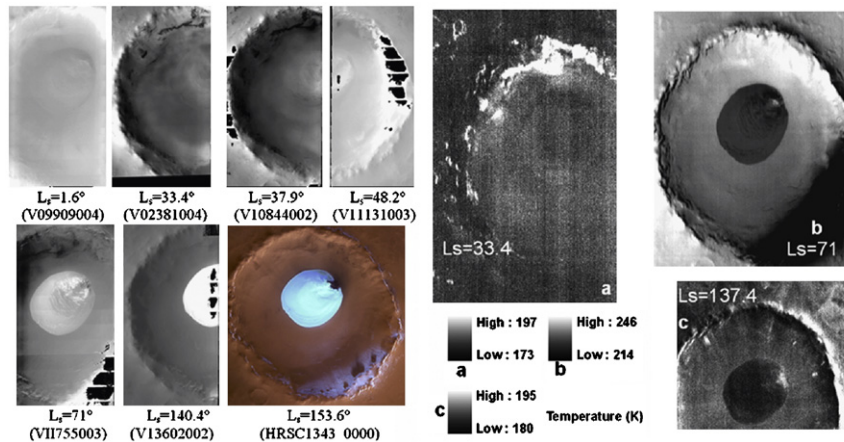


Fig. 5. Visible images of THEMIS and HRSC (left) and THEMIS brightness temperature images (right) of the 'Louth' crater (30 km in diameter). HRSC image courtesy ESA/Mars express (ESA/DLR/FU Berlin (G. Neukum)).

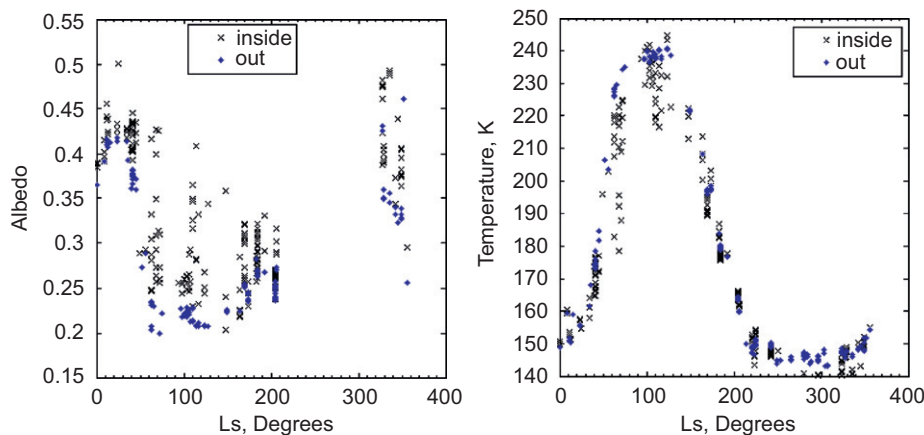


Fig. 6. TES-derived albedos (left) and bolometric temperature (right) measurements for both inside the Louth crater (x) and outside the Louth crater (●).

Since the water–ice is only a small portion of the crater interior (Fig. 5), it is difficult to retrieve the TES data for the exact ice location with no contamination from the regolith outside of the water–ice body. As a result, we only retrieve data for inside the crater ($70.0\text{--}70.327^\circ\text{N}$ and $256.19\text{--}257.246^\circ\text{W}$) and outside the crater ($70.83\text{--}71^\circ\text{N}$ and $258.49\text{--}257.68^\circ\text{W}$) as shown in Fig. 6. It is very clear that their albedo and temperature behaviors of both inside and outside the crater are similar during fall, winter, and early spring times, while they are different during the later spring to later summer times. The small water–ice is the reason for the lower temperature and higher albedos inside the crater compared with outside the crater, since there is no water–ice or frost outside the crater during later spring to later summer times when temperature are higher than 200 K. The starting time for the Phase 2 of this crater is around $L_s = 60^\circ$, a little later than that of the Korolev crater. Even the latitude of the 'Louth' crater is about 2° south of the Korolev crater, the 'Louth' crater is about 2 km in depth and 30 km in diameter compared with the 0.5–1 km in depth (majority of the crater) and 80 km in

diameter of the Korolev crater. This means that the Korolev crater is relatively wide open, compared with the 'Louth' crater, to receive more solar radiation, which could increase the temperature to 200 K faster and earlier than that of the 'Louth' crater. The ending time of the Phase 2 is around $L_s = 160^\circ$, similar as the Korolev crater. The trend of albedo change in the Phase 2 of the 'Louth' crater seen in the figure is slightly different from the conceptual model and the Korolev crater, mainly because its albedos are a mixed water–ice and regolith.

We believe that the water–ice on the central peak was a part of the water–ice body, left after the last polar ice recession of the last obliquity cycle, which once covered the entire crater floor. Sediments/dusts have been deposited on top of the water–ice since the last polar ice recession. Since the central peak of the crater is about 200–400 m higher than the rest of the crater floor, fewer sediments were deposited on it, while the rest of the crater floor has been almost fully covered by sediments/dusts. This explanation is supported by Brown et al. (2007), who used the high resolution imaging science experiment (HiRISE) image on

board the MRO to map the icy outliers of water–ice and suggest that the water–ice on the central peak may be a remnant of a previously larger extent of the ice deposit. They explain this as a result of ice melting (sublimates) due to possible global warming of Mars, against which we argue that the global warming should first melt (sublime) the water–ice on the central peak rather than the rest of the crater floor, since the peak should receive more solar radiation.

We examined two HiRISE images for this crater (Fig. 7). We found that the scattered small ice patches mentioned by Brown et al. (2007) only appeared in the HiRISE image 1 ($L_s = 137.4$) but not in the HiRISE image 2 ($L_s = 146.4$), even though their acquisition dates are very close. The northern portion of the crater floor is narrower than the southern portion of the crater floor, which may suggest that the northern portion could have received more deposits per unit area than that of the southern portion. This resulted in thick sediments on top of the water–ice in

the northern portion, which have helped to form a well-developed polygon and ice-wedge system (Fig. 7a, b), also known as a permafrost system. However, in the southwestern portion of the crater floor, due to less sediment received per unit area, the water–ice body is not fully covered and many small patches (1–6 m) are still exposed (Fig. 7c, d). This indicates an underdeveloped ice-wedge polygonal system; instead the cracks are mostly parallel and irregular.

4. Discussion

This paper proposes a conceptual model to explain the AM/PM HAEs related to crater-like features, in the north polar seasonal cap region. This model first requires a relatively permanent water–ice layer exposed in the crater interior. The icy layer (body) was the basis for the appearance of the HAEs in the Phase 2 during later spring to later summer, while the exact timing for each phase in different craters may vary depending on the temperature, since temperature is the dominated factor that not only controls the timings when dust starts thermally sinking, but also controls the timings when CO_2 and H_2O sublime and condense/deposit. Temperature itself is a function of elevation, depth, diameter, and location (especially latitude) of a crater. In Phase 1, the increase of albedo is probably mainly due to the decrease in aerosol optical thickness as sunrise over the polar region; the major process in this phase is the sublimation of CO_2 frost. In Phase 2, the first decrease of albedo is probably mainly due to dust contamination left in the Phase I, and then the increase of albedo is probably mainly due to that most dusts thermally sink into the water–ice and the exposing of H_2O frost. In this phase, cold-trapped water vapor could re-condense and deposit back onto the water–ice layer or crater floor in night time during middle to later summer season; but it will be the first to be sublimated during afternoon time, before the sublimation of previous year's water–frost and old water–ice. So this process will eventually exhaust all old water–ice if the total mass and extent of water–frost deposition (both current and previous years) is less than those of sublimation. In Phase 3, the decrease of albedo is probably mainly due to a mixed effect of exposing old water–ice and increasing aerosol thickness caused by dust storm. The origin of the H_2O frost for deposition in this phase is the atmospheric water vapor, mainly from the sublimation of polar water–ice in the Phase 2 period. In Phase 4, albedo will gradually increase due to deposition of CO_2 frost. The origin of the CO_2 frost in this phase is the atmospheric CO_2 .

For AM-only HAEs craters, there seems no need of a relatively permanent water–ice body or patches to be continuously exposed, so HAEs are not seen in PM time. But, the presence of a subsurface water–ice layer or ice-rich regolith is a necessary condition. High PM temperatures during later spring and summer seasons cause certain degrees of sublimation of the subsurface

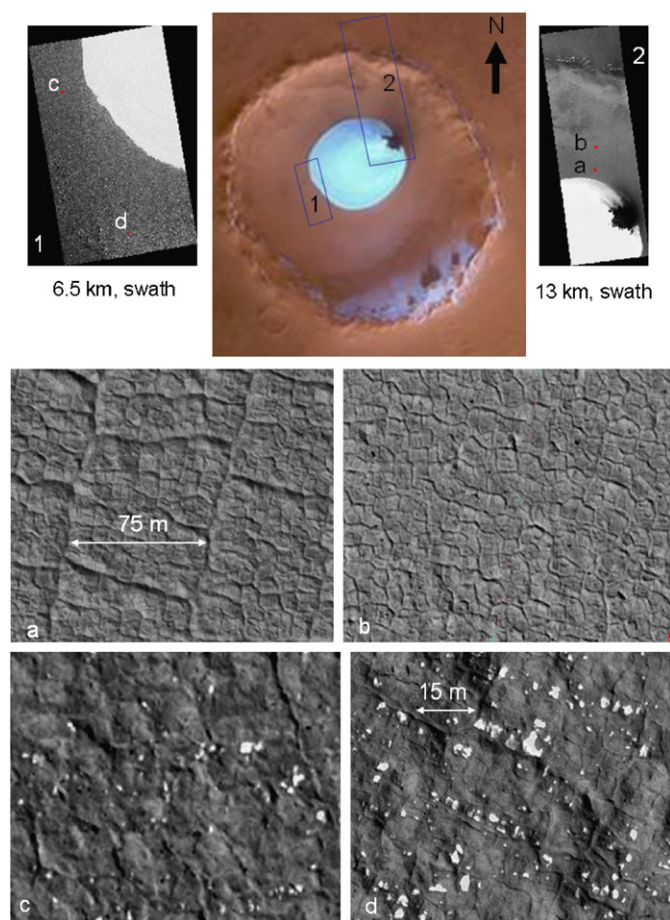


Fig. 7. Top panel is the index map showing the ‘Louth’ crater (HRSC Orbit 1343) and two HiRISE footprints and images (1: PSP001370_2505, $L_s = 133.7^\circ$ and 2: PSP001700_2505, $L_s = 146.4^\circ$). Subscene ‘a’ shows small polygons of 10–15 m across with ice-wedges of 1–2 m (young and shallow) bounded by larger ice-wedge (old and deep) of 3–5 m and polygon of 70–80 m across; ‘b’ shows small polygon and small ice-wedge network; and ‘c and d’ show small ice patches (1–6 m across) scattered in polygons of 6–9 m across, with ice-wedges of 1–2 m (few 3–4 m).

water–ice. The water vapor could be cold-trapped in the crater or near the crater, then re-condenses and deposits as water frost in night time when the temperature drops below the condensation temperature of water vapor, during middle to later summer season. Atmospheric water vapor, mainly from the sublimation of water–ice of the polar cap, might not be a source or a major source for the AM-only HAEs. Otherwise, all polar craters should have at least AM-only HAEs, which is not the case.

Since the origin of the crater water–ice bodies is hypothesized to remain from the last advance and recession of the polar cap margin since the last high-obliquity period, this model also projects that many crater-like features above 60° latitude should have water–ice exposed or water–ice nearly completely covered. This suggests that: (1) water–ice bodies, if existing but not currently exposed, should be very close to the floor surface of the crater-like features and (2) crater-like features, if they do not currently contain a water–ice layer exposed or covered, should be younger than the last episodic recession of the polar cap. Imagery studies of the crater morphologies and ages can be conducted to test this hypothesis. A similar model for the south polar region will also be established.

Acknowledgments

This work was partially supported by a NASA/Texas Space Grant Consortium New Investigations Program (#NNG05GE96H). The authors acknowledge the use of the MOC images from NASA/JPL/Malin Space Science Systems MOC images archive (MGS mission), THEMIS images and TES data from NASA/JPL/Arizona State University, HRSC image from ESA/Mars Express, and HiRISE images from NASA/JPL/University of Arizona. John Armstrong, who provided the TES data, is greatly appreciated. The authors would like to thank Y. Langevin, T.N. Titus, and an anonymous reviewer for their very helpful comments and suggestions that substantially improved this paper.

References

- Armstrong, J.C., Titus, T.N., Kieffer, H.H., 2005. Evidence for subsurface water ice in Korolev crater, Mars. *Icarus* 174, 360–372.
- Armstrong, J.C., Nielson, S.K., Titus, T.N., 2007. Survey of TES high albedo events in Mars' northern polar craters. *Geophys. Res. Lett.* 34.
- Bass, D.S., Herkenhoff, K.E., Paige, D.A., 2000. Variability of Mars' north polar ice cap: I. Analysis of Mariner 9 and Viking Orbiter imaging data. *Icarus* 144, 382–396.
- Bibring, J.P., et al., 2004. Perennial water ice identified in the South polar cap of Mars. *Nature* 428, 627.
- Bibring, J.P., et al., 2005. Mars surface diversity as revealed by the OMEGA/Mars express observations. *Science* 307, 1576–1581.
- Brown, A.J., et al., 2007. Evolution of water ice mound deposit in 'Louth' crater as observed by CRISM and HiRISE. In: Proceedings of the Lunar and Planetary Science Conference, 38th, Abstract 2262.
- Byrne, S., Ingersoll, A.P., 2003. Martian climate events on timescales of centuries: evidence from feature morphology in the residual south polar ice cap. *Geophys. Res. Lett.* 30, 1696.
- Cantor, B.A., James, P.B., Caplinger, M., Wolff, M.J., 2001. Martian dust storms: 1999 Mars Orbiter camera observations. *J. Geophys. Res.* 106 (E10), 23,653–23,688.
- Forget, F., et al., 1998. CO₂ snowfall on Mars: simulation with a general circulation model. *Icarus* 131, 302–318.
- Garvin, J.B., Frawley, J.J., 1998. Geometric properties of Martian impact craters: preliminary results from the Mars Orbiter Laser Altimeter. *Geophys. Res. Lett.* 25, 4405–4408.
- Garvin, J.B., et al., 2000. North polar craterforms on Mars: geometric characteristics from the Mars Orbiter Laser Altimeter. *Icarus* 144, 329–352.
- Hale, A.S., Bass, D.S., Tamppari, L.K., 2005. Monitoring the perennial Martian Northern polar cap with MGS MOC. *Icarus* 174 (2), 502–512.
- Kieffer, H.H., Kieffer, H.H., 1976. Soil and surface temperatures at the Viking landing sites. *Science* 194, 1344–1346.
- Kieffer, H.H., Titus, T.N., 2001. TES mapping of Mars' North seasonal ice cap. *Icarus* 154, 162–180.
- Langevin, Y., Poulet, F., Bibring, J.P., Schmitt, B., Doute, S., Gondet, B., 2005. Summer evolution of the North polar cap of Mars as observed by OMEGA/Mars express. *Science* 307, 1581–1584.
- Langevin, Y., Bibring, J.-P., Montmessin, F., Forget, F., Vincendon, M., Doute, S., Poulet, F., Gondet, B., 2007. Observations of the South seasonal cap of Mars during recession in 2004–2006 by the OMEGA visible/near-infrared imaging spectrometer on board Mars express. *J. Geophys. Res.* 112, E08S12.
- Leighton, R.R., Murray, B.C., 1966. Behavior of carbon dioxide and other volatiles on Mars. *Science* 153, 136–144.
- Tillman, J.E., et al., 1993. The Martian annual atmospheric pressure cycle: years without great dust storms. *J. Geophys. Res.* 98, 10963–10971.
- Titus, T.N., 2003. CO₂ cycle: two martian years of polar IR observations. In: Workshop on Mars Atmosphere Modeling and Observations. Granada, Spain January 13–15.
- Titus, T.N., Kieffer, H.H., Christensen, P.R., 2003. Exposed water ice discovered near the South pole of Mars. *Science* 299, 1048–1051.
- Vincendon, M., Langevin, Y., Poulet, F., Bibring, J.P., Schmitt, B., Doute, S., OMEGA team, 2006. Surface water ice and aerosols evolution of 77N, 90E Mars crater during early summer by OMEGA/MEX. In: Proceedings of the Lunar and Planetary Science Conference, 37th, Abstract 1769.
- Vincendon, M., Langevin, Y., Poulet, F., Bibring, J.-P., Gondet, B., 2007. Recovery of surface reflectance spectra and evaluation of the optical depth of aerosols in the near-IR using a Monte Carlo approach: application to the OMEGA observations of high-latitude regions of Mars. *J. Geophys. Res.* 112, E08S13.
- Xie, H., Zhu, M., Guan, H., Smith, R.K., 2006. Isolated water ice in an unnamed crater away from the residual north polar cap of Mars: The only one? In: Proceedings of the Lunar and Planetary Science Conference, 37th, Abstract 1764.